DETECTION OF PERIODIC CLIMATE ANOMALIES OVER GREENLAND WITH MICROWAVE RADIOMETERS

Wolfgang Wagner[1], Per Gloersen[2]
[1] Student, Institute for Photogrammetry and Remote Sensing, Vienna University of Technology
[2] Senior Scientist, Oceans and Ice Branch, Laboratory for Hydrospheric Processes, NASA Goddard Space Flight Centre

Commission VII, Working Group 8

KEY WORDS: Radiometry, Change Detection, Spectral Analysis, Greenland, Ice Sheet

ABSTRACT

We investigate the potential of microwave radiometers for the detection of periodic climate anomalies over Greenland. A multiple-window harmonic analysis technique is applied to a nine year record of Scanning Multichannel Microwave Radiometer (SMMR) data. We concentrated on the 37GHz vertically polarized channel to obtain a good correlation between the signal and ice crystal size over the skin depth. Year to year differences in microwave emission from the percolation facies of the Greenland Ice Sheet are explained by the absence or varying degree of surface melt during summer. Quadrennial oscillations were found to occur more frequently in the brightness temperature record than oscillations with periods of one or two years.

1. INTRODUCTION

The Greenland ice sheet is the largest ice sheet in the Northern Hemisphere. The present ice sheet has a surface area of 1,750,000 km^2 (Steffen et al., 1993), that is twenty one times the size of Austria and roughly the size of Mexico. Little is yet known about the Greenland ice sheet despite its important role for climate studies and for climate itself (Thomas, 1993). Research has been hampered by its vast size and the harshness of the polar environment. Remote sensing satellites are able to provide measurements over large areas and will thus contribute to our understanding of the Greenland ice sheet. The usefulness of microwave radiometers, like the Scanning Multichannel Microwave Radiometer (SMMR), for the study of the polar ice sheets has already been demonstrated. The most prominent application of microwave radiometers is detection of surface melting on the ice sheets. Since moisture in the near-surface firn causes a marked increase in microwave brightness temperatures (T_b), very high values of T_b indicate surface melting. Thereby the extent and duration of surface melting can be derived. Presently long term-series of such information are being established (Zwally and Fiegels, 1994).

In this study we investigated the potential of microwave radiometers for the detection of periodic climate anomalies over Greenland. By studying the spatial and temporal variabilities of geophysical parameters, global patterns can be depicted which makes it possible to link weather and climate anomalies in one region of the globe to another (Lau and Busalacchi, 1993; Gloersen, 1995).

2. METHOD

To find periodic signals in the microwave emission from the Greenland ice sheet we applied a novel harmonic analysis technique to a nine year record of SMMR brightness temperatures. The harmonic analysis technique was developed for investigating seismic, atmospheric carbon dioxide, and other time series records (Park et al., 1987; Kuo et al. 1990). Several names can be found for it in the literature. We will refer to this technique as the „multiple-window harmonic analysis". The multiple-window harmonic analysis aims for finding the harmonic components of a time series. The method is novel in that it uses several windows to fit a sinusoid model to the data and that it utilizes a F-test statistic to test the fit of the sinusoid model.

We analyzed data from the Scanning Multichannel Microwave Radiometer (SMMR) which was operated on board of the Nimbus 7 satellite from October 26, 1978 to August 20, 1987. The SMMR is a 10-channel instrument receiving both horizontally (H) and vertically (V) polarized radiation at 5 frequencies. Only the 37 GHz V and H channels were considered because of the greater sensitivity of the 37 GHz data to near-surface changes compared to the longer-wavelength data (Schuman et al., 1995). The spatial resolution of the data at 37 GHz is approximately 30 km. The SMMR instrument was generally operated on an every-other-day basis. Our data set thus comprised 1611 images for both the 37 GHz vertically polarized channel and the 37 GHz horizontally polarized channel. The SMMR data have been mapped onto a rectangular grid with a grid cell size of 25 km x 25 km over a stereographic projection. For a detailed description of the SMMR see Gloersen et al. (1992).

Brightness temperature time series were established for each grid cell. The time series were detrended assuming that the trend is linear. Following the procedures described in the Appendix „Multiple-window harmonic analysis" we calculated the complex amplitude, μ, of the sinusoid model and the F-test parameter, F, from the detrended data. The sum over time is taken on six-day intervals instead of the original two-day intervals to match the revisit time of the SMMR. The complex amplitude gives information about the magnitude and phase of the sinusoid model immersed in the time series, and the F-test

parameter allows us to determine the probability that there are coherent oscillations in the data. Both parameters can be calculated at any frequency. For convenience the frequency f of an oscillation will be expressed in terms of the period $\tau=1/f$ in years.

3. MICROWAVE EMISSION FROM DRY FIRN

Microwave emission from dry firn depends on the physical temperature of the snow and on the snow morphology over the skin depth. According to Rott et al. (1993) the skin depth at 37 GHz is approximately 0.85 m. The observed brightness temperatures over ice sheets are less than expected from a black-body radiating at the in-situ temperature because of volume scattering over the skin depth, and because of reflection of radiation from below at the snow-air interface (Remi and Minister, 1991). Any energy that is scattered or reflected downward is not emitted, so scattering and reflection decrease the observed brightness temperature.

The scattering efficiency of a layer of snow is strongly dependent on the size distribution of the ice crystals. According to electromagnetic wave theory the scattering efficiency of ice grains increases with grain size. Dense medium radiative transfer theory has shown that the larger ice grains in a snow layer are responsible for most of the scattering (West et al., 1993). The emissivity of a layer of coarse snow or of a refrozen crust is thus smaller than the emissivity of a layer of new snow (Mätzler, 1987).

Downward reflection at the snow-air interface depends on surface roughness, surface density, incidence angle, and polarization (Remi and Minister, 1991). Coarse grained hoar layers on the surface of the ice sheet reduce the near surface density and increase surface roughness at approximately the scale of 37 GHz wavelength (Shuman et al., 1993). This creates a surface which reduces H reflection with the result that brightness temperature in H-band might increase despite larger ice grains. On the other hand, V-reflection increases, adding energy to downward scattering by the coarse ice grains. Thus the V-signal always decreases during the formation of hoar complexes.

Initially all computations were performed for both polarizations. Basically the results are very similar, but there are some differences that cannot be easily explained. We finally decided to concentrate on V-band because we followed the idea that meteorological conditions influence ice crystal growth. To obtain a good correlation between the signal and ice crystal size over the skin depth, the 37 GHz vertically polarized channel seems to be the right choice. In addition, the V-signal is less noisy than the H-signal.

4. RESULTS AND DISCUSSION

Maps of the absolute value of the complex amplitude, $|\mu|$, and the F-test parameter, F, were computed for various periods. Interannual variations in microwave emission from the ice sheet are depicted in the maps for periods $\tau=2,3$, and 4 years. To investigate oscillations with a period greater than four years does not make much sense for a nine year record. Interestingly, quadrennial oscillations can be found over much larger portions of Greenland than biennial and triennial variations, and $|\mu|$ and F are generally higher for the former one.

In Figure 1 $|\mu|$ and F of the quadrennial oscillation are plotted onto the shape of Greenland. The boundaries in the interior of Greenland define the dry-snow facies and the percolation facies according to Benson (1962). The dry-snow facies corresponds to the deep interior of the ice sheet and is characterized by the absence of seasonal melt. In the percolation zone vigorous melting may occur near the surface. Ice pipes and massive ice lenses are found in these regions as well as strong seasonal modulation of ice grain size (Jezek et al., 1994). In the dark colored patches of Figure 1a the F-test parameter is above the 99 % confidence level at 6.51. With the exception of small clusters along the coast of Greenland, the F-test statistics shows that the quadrennial signal can predominately be found above the saturation line (Below the saturation line the ice sheet surface becomes wet throughout the melting season). As evident in Figure 1b high values of $|\mu|$ are mainly found in the percolation zone.

We now try to answer the question what caused the four-year signal in the brightness temperature record? Let us have a look at some time series of T_b from selected points on the ice sheet. These points are numbered from 1 to 6 and their location can be seen in Figure 1. The corresponding time series are displayed in Figure 2. Comparing time series from the percolation zone (1-5) we find that while summer brightness temperatures are always rather similar, winter brightness temperatures can vary significantly. This is most evident in the brightness temperature record from point 1. There T_b varies up to 40 K between different winters. High T_b peaks in the summers of 1981 and 1985 indicate surface melt. Since surface melt usually results in layers of iced firn consisting of clusters of grains bonded together by frozen melt water (Benson, 1962), we think that the high differences in brightness temperature measurements between the winters must be explained by differences in the ice grain size distribution. According to Benson (1962) grains in firn strata which have not been exposed to melt action are predominantly less than 1 mm. Grains exposed to temperatures within about 5 degree of melting, but not soaked, fall in the medium size range, between 1 and 2 mm. When surface melt and soaking occur, individual grains are primarily larger than 2 mm and cluster may exceed 5 mm. The size range of the individual scatterers is thus large (0.1 to 5 mm). Ice grain size might therefore serve as an index for the past climate.

New snow that buries a layer of coarse snow increases brightness temperature. As long as the depth of the new snow layer is low in comparison the skin depth (0.85 m), there is always significant contribution to the signal from the coarse snow layer below the surface. The relatively slow increase in T_b at point 1 in the winters of 1981/82 and 1985/86 suggests that winter accumulation was relatively low. According to Ohmura and Reeh (1991) annual accumulation in the surroundings of point 1 is around 500 mm water equivalent. Assuming a snow density of 0.2 g/cm^3 annual accumulation expressed in snow depth is estimated to be around 2.5 m. Considering the natural variability in precipitation and precipitation minimum in winter (Bromwich et al., 1993) it

does not seem improbable that the coarse summer layer kept microwave emission low for most of the winter period.

We think microwave emission from points 2 to 5 can be explained in a very similar fashion. (For the interpretation of these time series one should keep in mind that above normal T_b indicates surface melting.) From all this we conclude that interannual variabilities in microwave emission from the percolation facies can mainly be explained by the absence or varying degree of surface melting during the summer. This conclusion is based only on deductive reasoning, since we had no field observations for comparison with our data.

The cause for the quadrennial oscillation at point 6 which is located in the dry-snow facies is different: T_b follows the seasonal trend and there is no indication for surface melt. Since we can only speculate about the reason why the annual average of T_b is slowly varying, we will not provide an explanation.

5. CONCLUSIONS

We think that year to year differences in microwave emission from the percolation facies of the Greenland Ice Sheet are mainly due to various degrees of melting during summer. If this hypothesis holds true then the frequency of climate anomalies during the melting season can be assessed over the percolation zone of the Greenland Ice Sheet by applying harmonic analysis techniques to passive microwave data. We used a multiple-window harmonic analysis technique to analyze the 37GHz channels of the SMMR. This technique allows to see spectral components very clearly. Quadrennial oscillations were found to occur more frequently in the brightness temperature record than biennial and triennial oscillations.

REFERENCES

Benson, C.S., 1962. Stratigraphic studies in the snow and firn of the Greenland Ice Sheet. Res. Reps. 70, U.S. Army, SIPRE (now CRREL), Hanover, NH

Bromwich, D.H., F.M. Robasky, R.A. Keen, J.F. Bolzan, 1993. Modeled variations of precipitation over the Greenland Ice Sheet. J. Climate, 6, pp. 1253-1268.

Gloersen, P., 1995. Modulation of hemispheric sea-ice cover by ENSO events. Nature, 373, pp. 503-506.

Gloersen, P., W.J. Campell, D.J. Cavalieri, J.C. Comiso, C.L. Parkinson, H.J Zwally, 1992. Arctic and Antarctic Sea Ice, 1978-1987: Satellite Passive-Microwave Observations, NASA SP-511, National Aeronautics and Space Administration, Washington, DC.

Jezek, K.C., P. Gogineni, M. Shanableh, 1994. Radar measurements of melt zones on the Greenland Ice Sheet. Geophys. Res. Letters, 21(1), pp. 33-36.

Kuo, C., C. Lindberg, D. Thomson, 1990. Coherence established between atmospheric carbon dioxide and global temperature. Nature,343, pp. 709-713.

Lau, K.M., A.J. Busalacchi, 1993. El Niño Southern Oscillation: a view from space, in Atlas of satellite observations related to global change. R.J. Gurney, J.L Foster, C.L. Parkinson (eds.), Cambridge University Press

Lindberg, C.R., J. Park, 1987. Multiple-taper spectral analysis of terrestrial free oscillations: part II. Geophys. J. R. astr. Soc., 91, pp. 795-836.

Mätzler, C., 1987. Applications of the interaction of microwaves with the natural snow cover. Remote Sensing Rev., 2, pp. 259-387.

Ohmura, A., N. Reeh, 1991. New precipitaion and accumulation maps for Greenland. J. Glaciol., 37(125), pp. 140-148.

Park, J., C.R. Lindberg, D.J. Thomson, 1987. Multiple-taper spectral analysis of terrestrial free oscillations: part I. Geophys. J. R. astr. Soc., 91, pp. 755-794.

Remy, F., J.F. Minister, 1991. A comparison between active and passive microwave measurements of the Antarctic ice sheet and their association with the surface katabatic winds. J. Glaciol., 37(125), pp.3-10.

Rott, H., K. Sturm, H. Miller, 1993. Active and passive microwave signatures of Antarctic firn by means of field measurements and satellite data. Ann. Glac., 17, pp. 183-188.

Shuman, C.A., R.B. Alley, S. Anandakrishnan, 1993. Characterization of a hoar-development episode using SSM/I brightness temperatures in the vicinity of the GISP2 site. Greenland, Ann. Glac., 17, pp. 183-188.

Steffen, K., W. Abdalati, J. Stroeve, 1993. Climate sensitivity studies of the Greenland Ice Sheet using satellite AVHRR, SMMR, SSM/I and In Situ data. Meteorol. Atmos. Phys., 51, pp. 239-258.

Thomas, R.H., 1993. Ice sheets. in Atlas of satellite observations related to global change, R.J Gurney, J.L. Foster, C.L. Parkinson (eds.), Cambridge University Press.

Thomson, D.J., 1982. Spectrum estimation and harmonic analysis. Proc. IEEE, 70(9), pp. 1055-1096.

Zwally, H.J., S. Fiegels, 1994. Extent and duration of Antarctic surface melting. J. Glaciol., 40(136), pp. 463-476.

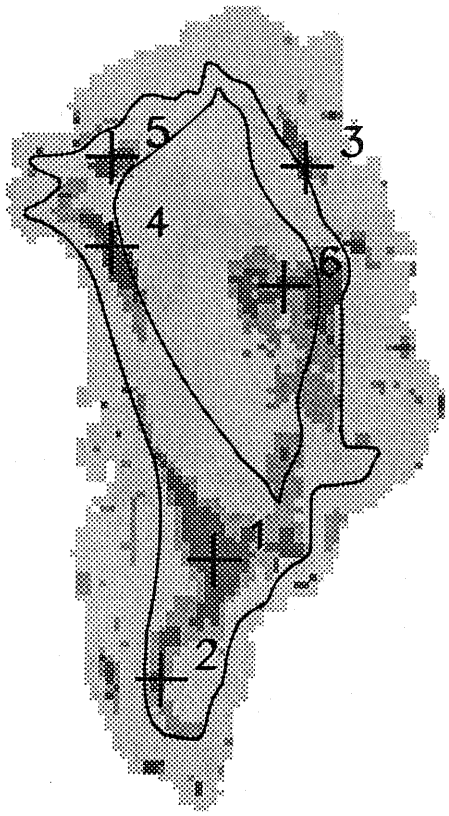

Figure 1a. F-test parameter, F, for period τ=4yr. F was calculated by applying a multiple-window harmonic analysis technique to SMMR 37GHz vertically polarized T_b. The two boundaries define the dry-snow facies and the percolation facies according to Benson (1962).

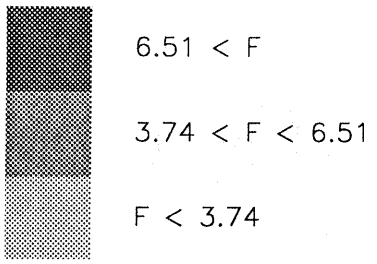

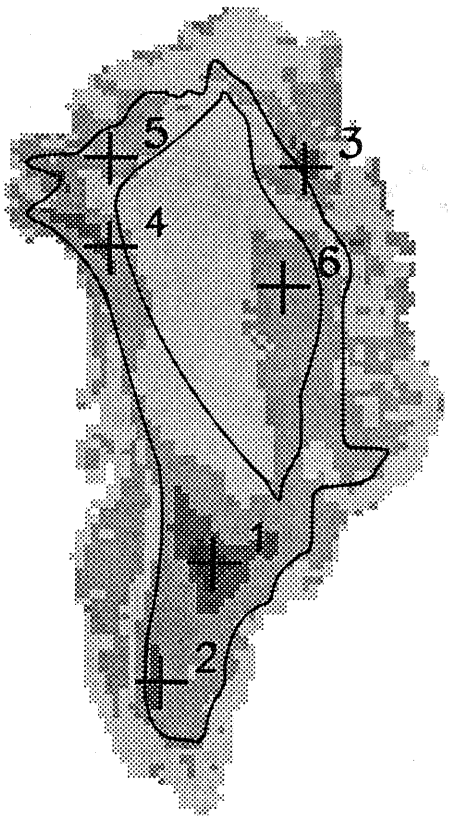

Figure 1b. Absolute value of complex amplitude, $|\mu|$, for period τ=4yr. $|\mu|$ was calculated by applying a multiple-window harmonic analysis technique to SMMR 37GHz vertically polarized T_b. The two boundaries define the dry-snow facies and the percolation facies according to Benson (1962).

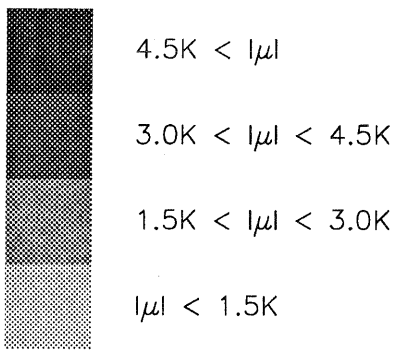

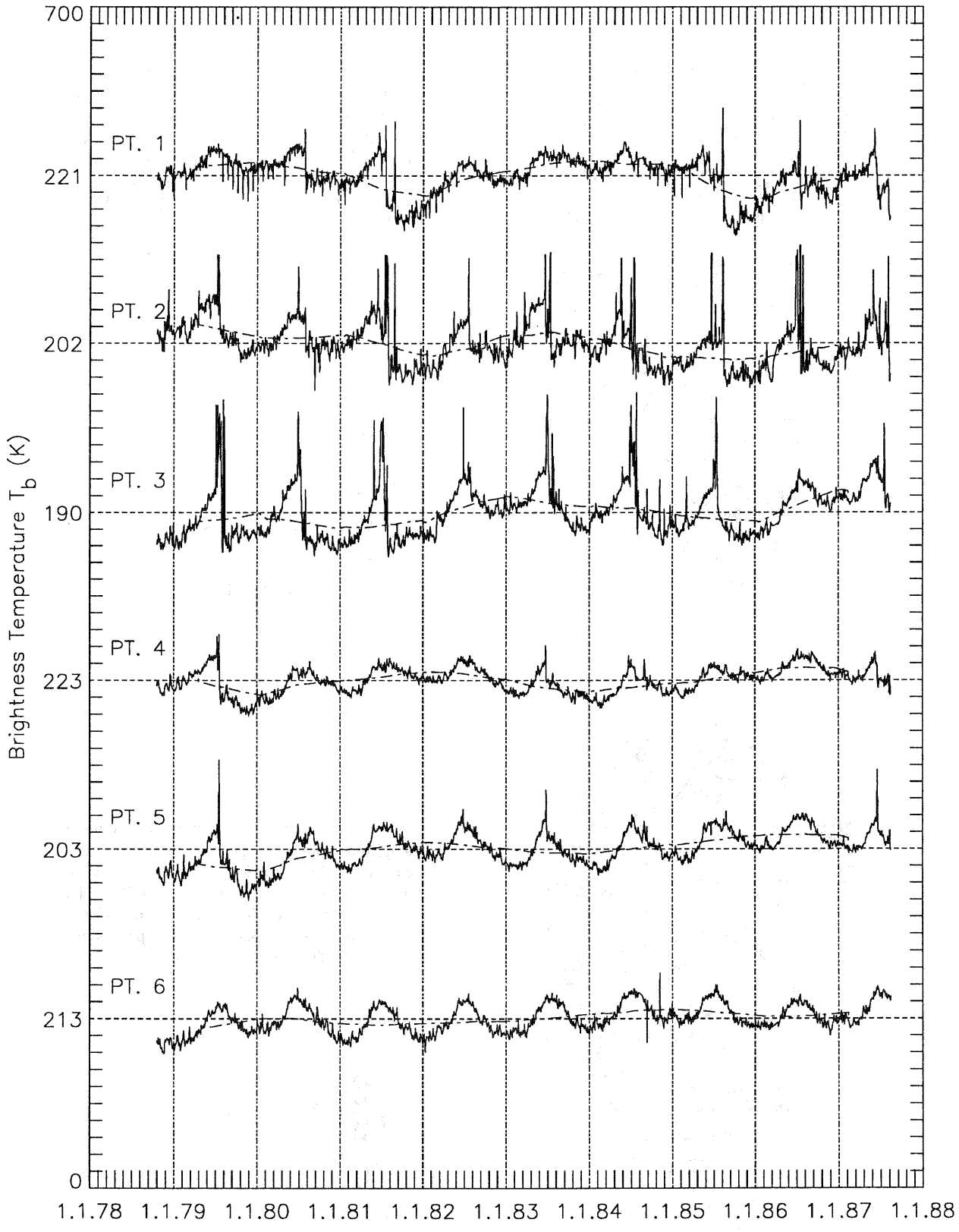

Figure 2. Time series of T_b together with the running annual averages from October 26, 1978 to August 20, 1987 at six locations on the Greenland Ice Sheet (cf. Figure 1). The grid spacing of the T_b axis is equal to 10 K. The numbers on the T_b axis represent average brightness temperatures of the individual time series.

APPENDIX: MULTIPLE-WINDOW HARMONIC ANALYSIS

We shortly summarise the basic assumptions and formulas of this multiple-window harmonic analysis technique which was introduced by Thomson (1982) and extended by Park et al. (1987), Lindberg and Park (1987).

The purpose of an harmonic analysis is the detection of spectral harmonic line components and the measurement of their frequencies and amplitudes. It is assumed that the spectrum of a time-series x(t) consist of harmonic line components and a continuous background spectrum. In the frequency interval (f+W,f-W) with sufficiently small values of W the record x(t) can be written

$$x(t) = \mu e^{i2\pi ft} + e(t) \tag{1}$$

where μ is a complex amplitude and e(t) is an error term. The error term e(t) consist of other sinusoids and noise. In practice we have N measurements of x(t). The time between successive samples is assumed to be 1 so that the frequency f is defined on its principal domain (-1/2,1/2].

K different complex eigenspectra $y_k(f)$ are produced in the frequency domain by the discrete Fourier transformations

$$y_k(f) = \sum_{t=0}^{N-1} e^{-i2\pi ft} x(t) v_k(t) \qquad k=0,1,..,K-1 \tag{2}$$

where the $v_k(t)$ are the discrete prolate spheroidal sequences. The discrete prolate spheroidal sequences $v_k(t)$ can be calculated by taking a singular value decomposition of a sinc matrix and are optimal windows for concentrating the energy of sinusoids in the frequency interval (f+W,f-W). They maximise the functional

$$\frac{\int_{f-W}^{f+W} |y_k(\nu)|^2 \, d\nu}{\int_{-1/2}^{1/2} |y_k(\nu)|^2 \, d\nu}. \tag{3}$$

With W chosen to be 4/N the functional (3) has a value close to one for the first eight discrete prolate spheroidal sequences $v_0(t)$, $v_1(t)$, .., $v_7(t)$, and rapidly drops off thereafter. Since only $v_k(t)$ with good spectral leakage resistance should be considered in the computations, we set K equal to 8.

The absolute squares of $y_k(f)$

$$S_k(f) = |y_k(f)|^2 \qquad k=0,1,..,K-1 \tag{4}$$

can be regarded as individually direct spectrum estimates. However, the novelty of the multiple taper method is that is utilises more data than conventional methods by using all complex eigenspectra $y_k(f)$ with good spectral leakage resistance. Applying regression techniques to the $y_k(f)$ an estimate of the complex amplitude μ is obtained

$$\hat{\mu}(f) = \frac{\sum_{k=0}^{K-1} V_{0k} y_k(f)}{\sum_{k=0}^{K-1} V_{0k}^2} \tag{5}$$

where

$$V_{0k} = \sum_{t=0}^{N-1} v_k(t). \tag{6}$$

The multiple-window method also provides a statistical F-test to test the fit of the sinusoid model. The random variable

$$F(f) = \frac{(K-1)|\hat{\mu}(f)|^2 \sum_{k=0}^{K-1} V_{0k}^2}{\sum_{k=1}^{K-1} |y_k(f) - \hat{\mu}(f) V_{0k}|^2} \tag{7}$$

follows an F-distribution with 2 and 2K-1 degrees of freedom. For significance level γ the hypothesis $\mu=0$ is rejected if $F(f) \geq F_{2,2K-1;1-\gamma}$. In our case (K=8) the 95% confidence level of the f-test statistic is at 3.74 and the 99% confidence level is at 6.51.